Indian Journal of Biochemistry & Biophysics
Vol. 62, July 2025, pp. 743-753
DOI: 10.56042/ijbb.v62i7.16439

Identification of hub genes in monocyte macrophages of high and low peak bone mass populations and early diagnostic biomarkers for osteoporosis

Jing Xiao[1], Rui Ding[1], Zhiyuan Xu[2], Zhiwei Deng[2], Juntong Xie[2] & Yiyan Qiu[1,2]*

[1]Academy of Orthopedics, Guangdong Province, Guangdong Provincial Key Laboratory of Bone and Joint Degeneration Diseases, Department of Orthopedics, The Third Affiliated Hospital, Southern Medical University, Guangzhou-510 630, China

[2]Department of Orthopedics, Central Laboratory of Longgang District People's Hospital of Shenzhen & The Second Affiliated Hospital, The Chinese University of Hong Kong, Shenzhen-518 172, China

Received 16 January 2025; *revised 11 March 2025*

Osteoporosis (OP) , a degenerative condition defined by osteopenia, is strongly influenced by peak bone mass (PBM) . However, the early diagnosis of osteoporosis remains incompletely understood. This study aims to identify early diagnostic biomarkers in populations with low PBM and to validate their clinical significance in the diagnosis, treatment, and prevention of osteoporosis. We obtained three microarray datasets (GSE2208, GSE97498, and GSE64433) from the Gene Expression Omnibus (GEO) database. Differentially expressed genes (DEGs) were screened using the limma package. Gene Ontology (GO) enrichment and Kyoto Encyclopedia of Genes and Genomes (KEGG) pathway analysis were performed. Protein-protein interaction network (PPI) analysis and visualization were conducted with String and Cytoscape. CytoHubba was used to identify hub genes, and relevant miRNAs were predicted using CyTargetLinker in Cytoscape. Finally, the hub genes and predicted miRNA expression were confirmed via RT-qPCR experiments in peripheral blood monocytes of ovariectomy (OVX) mice. We identified 747 DEGs from GSE2208 and 1238 DEGs from GSE97498 and identified 58 overlapping DGEs between these two datasets. The enriched GO terms and pathways were determined, including "TNF signaling pathway, plasma membrane, protease binding, and positive regulation of I-κB kinase/NF-κB signaling." Ten hub genes (TNF, FN-1, CCR2, HB-EGF, MMP14, NOD2, SOCS3, IFNAR1, IRAK3, PRKACB) were selected from the overlapping DEGs. Additionally, 42 target miRNAs were identified for the ten hub genes using CyTargetLinker. Eight miRNAs were selected after cross-validation with the osteoporosis miRNA expression profiling dataset (GSE64433) . In RT-qPCR experiments, the ten hub genes and eight predicted miRNAs in the blood monocytes of OVX mice were further validated. The study found that the hub genes and predicted miRNAs are potentially linked to OP development and may serve as biomarkers for the early screening of individuals at high risk of OP, thus playing a pivotal role in OP prevention and treatment. This provides a valuable foundation for further experimental studies and clinical applications.

Keywords: Bioinformatics analysis, Differentially expressed gene, miRNA, OVX

OP is a prevalent bone disease marked by reduced bone mass and compromised tissue structure, leading to heightened fracture risk and bone fragility[1]. Based on 2010 statistics from the Chinese Center for Disease Control and Prevention, osteoporosis affected 11.4 million people in China and is expected to exceed 212 million by 2050[2]. With the increasing problem of an ageing population, OP has become a global public health problem, and the incidence associated with OP is increasing. OP represents a significant threat to public health, particularly among middle-aged and elderly populations[3].

Peak bone mass, the maximum bone density attained during growth (usually by ages 30 to 35) , is a key determinant in developing OP and fractures in adulthood[4]. After achieving peak bone mass, adults steadily decline in bone density each year. Research indicates that individuals with low PBM have a higher risk of osteoporosis, whereas those with higher PBM can delay OP onset due to more substantial bone reserves[5]. With a 10% rise in PBM, the likelihood of fractures after age 50 drops by 50%[6,7]. Therefore, strategies to increase PBM during adolescence to enhance bone reserves for later life have become prominent research.

Bone homeostasis is the dynamic balance between osteoblasts and osteoclasts[8]. An imbalance between these processes and abnormalities occurs in bone structure and function, leading to postmenopausal and secondary OP[9]. Osteoclast differentiation is regulated by several factors, including nuclear factor of

*Correspondence:
E-mail: YiyanQiu_123@hotmail.com

activated T cells 1 gene (NFATc1) , macrophage colony-stimulating factor, ligand of receptor activator of NF-κB (RANKL) , osteoprotegerin, c-Fos, and tumor necrosis factor receptor-associated factor 6[10]. Abnormal OC activity contributes to bone defects, especially as their excessive activation is usually associated with many pathologies, hormonal imbalances, and hormone-based drug treatments[11,12]. Increased bone degradation due to OCs results in progressive bone loss. However, the mechanisms by which osteoclasts contribute to OP are not yet completely understood. Investigating the genes involved in OP and their interactions within molecular networks could uncover novel markers and targets for its prevention, diagnosis, and treatment.

In this study, cross-validation of DEGs was conducted in monocytes from low-PBM individuals and human peripheral blood CD14+ monocytes with derived macrophages (MACs) and OCs. These genes were used for PPI analysis, and highly connected hub genes were identified, along with GO and KEGG enrichment analyses. Furthermore, we constructed an mRNA-miRNA network. RT-qPCR experiments were conducted to confirm the hub genes and predicted miRNA expression *in vivo.*

Materials and Methods

Data sources

Microarray data were searched using the high-throughput GEO database in NCBI (https://www.ncbi.nlm.nih.gov/geo/) [13]. The dataset GSE97498 is based on the GPL13607, consisting of RNA expression profiles of human peripheral blood CD14+ monocytes with derived macrophages (MACs) and OCs. The dataset GSE2208 is based on the GPL96, which collected monocytes isolated from 30 mL of whole blood from 19 women, including 9 with low bone mineral density (BMD) and 10 with high BMD. The miRNA expression profile GSE64433 included 48 samples of 23 postmenopausal osteoporosis patients and 25 postmenopausal without osteoporosis controls.

Data processing

Data preprocessing and differential expression analysis were obtained by downloading the dataset data from the GEO website and obtaining the gene expression matrix files. DEGs were conducted using the limma package in R software[14]. The P value < 0.05 and | logFC | >0.5 were considered significant DEGs.

GO enrichment and KEGG pathway analysis of the DEGs

Gene Ontology and KEGG pathway enrichment analyses were performed using the online website DAVID (https://davidbioinformatics.nih.gov/) to clarify the biological roles of the screened differential genes. GO is divided into three components: biological process (BP) , cellular component (CC) , and molecular function (MF) . The P value <0.05 was considered statistically significant.

PPI network analysis and hub genes identification

The PPI network analysis of DEGs was performed by the online website String (https://www.string-db.org/) , set to remove unconnected nodes, and PPI network visualization mapping and PPI network annotation files were obtained[15]. The annotation file was loaded into Cytoscape (version 3.10.1) , and the MCC algorithm in the CytoHubba plugin was applied to calculate node scores in the network; the top ten ranked genes were identified as hub genes[16]. Then, the visualization of key gene PPI networks was performed.

miRNA-gene regulatory module prediction

The CyTargetLinker in Cytoscape (v3.8.2) was used to identify potential regulatory connections between the top 10 hub genes and miRNAs. The predicted miRNAs were then validated by intersecting them with differentially expressed miRNA (DE-miRNA) from the GSE64433 dataset.

OVX model construction

Sixteen healthy, 8-week-old female C57BL/6 mice were obtained from Guangdong Carrot Animal Company. C57BL/6 mice were randomly divided into the OVX group and the sham-operated (SHAM) group (n = 8) . After 3 weeks in the experimental animal center, bilateral OVXs and sham operations were performed. Twelve weeks post-surgery, blood and femur samples were preserved for testing after euthanizing the mice. The institutional animal care approved this experiment and use committee at Southern Medical University.

Micro-CT scanning and analysis

The femurs were dissected, cleaned, and fixed in 4% paraformaldehyde for 48 h. A micro-CT scanner (Viva CT40, Switzerland) was used to scan and analyze the specimens. Scanning parameters were configured as 160 kV voltage, 500 mA current, and 12 μm/pixel resolution. The region of interest (ROI) was defined as the trabeculae located 0.5 mm to

1.5 mm below the distal growth plate of the mouse femur. 3D structures were reconstructed. BMD and bone volume fraction (BV/TV) were evaluated.

Quantitative real-time PCR experiments

RNA, including miRNA, was isolated from mice peripheral blood using TRIzol® reagent (Invitrogen, USA) . RNA was reverse transcribed for mRNA extraction using the PrimerScript™ RT Kit (TaKaRa, China) , and miRNA was obtained with the SYBR® PrimeScript™ miRNA RT-PCR Kit (TaKaRa) . RNA extraction and reverse transcription followed the protocols provided by the manufacturer. RT-qPCR for mRNA was conducted on the Roche LightCycler® 96 Real-Time PCR System (Roche, Switzerland) using the SYBR® Premix Ex Taq™ RT-PCR Kit (TaKaRa) . The SYBR® PrimeScript™ miRNA RT-PCR Kit was used for miRNA quantification by qRT-PCR on the Roche LightCycler® 96 Real-Time PCR System. Amplification steps followed the protocols outlined by the manufacturer. Each sample was tested in triplicate, and relative expression was determined from Ct values via the ΔΔCt method. GAPDH was used to normalize mRNA expression, and U6 served as the reference for miRNA normalization. Primer sequences are provided in (Table 1) .

Statistical analysis

SPSS 26.0 software was used for statistical analysis. Results are expressed as mean ± standard deviation. A Student's *t*-test (unpaired, two-tailed) was applied to compare differences between two independent groups. All tests were performed independently, with each test conducted at least three times. A P-value of < 0.05 was considered statistically significant unless stated otherwise.

Results

Identification and Enrichment of DEGs Between Low-PBM Monocytes and High-PBM Monocytes

The dataset GSE2208 contains ten high-BMD and nine low-BMD samples. To obtain the most significant DEGs, the data were processed using the Limma package, resulting in the identification of 477 up-regulated and 270 down-regulated genes under the defined criteria. GO and KEGG enrichment analyses of the DEGs were conducted using DAVID. The top 5 results are presented in (Fig. 1A-C) , including the top five BP: mRNA splicing via spliceosome, mRNA transport, positive regulation of transcription from RNA polymerase II promoter, transcription, DNA-templated, RNA splicing; MF: protein binding, RNA binding, ATP binding, mRNA binding, enzyme binding; and CC: nucleoplasm, cytosol, cytoplasm, nucleus, nuclear speck. The top five KEGG pathways were protein processing in the endoplasmic reticulum, spliceosome, nucleocytoplasmic transport, estrogen signaling pathway, and hepatitis B (Fig. 1D) .

Table 1 — The primers used for PCR

Gene Name	Forward primer (5′- 3′)	Reverse primer (5′- 3′)
CCR2	ATCCACGGCATACTATCAACATC	CAAGGCTCACCATCATCGTAG
NOD2	CAGGTCTCCGAGAGGGTACTG	GCTACGGATGAGCCAAATGAAG
SOCS3	ATGGTCACCCACAGCAAGTTT	TCCAGTAGAATCCGCTCTCCT
HBEGF	CGGGGAGTGCAGATACCTG	TTCTCCACTGGTAGAGTCAGC
IFNAR1	AGCCACGGAGAGTCAATGG	GCTCTGACACGAAACTGTGTTTT
IRAK3	CTGGCTGGATGTTCGTCATATT	GGAGAACCTCTAAAAGGTCGC
TNF	CCCTCACACTCAGATCATCTTCT	GCTACGACGTGGGCTACAG
FN1	ATGTGGACCCCTCCTGATAGT	GCCCAGTGATTTCAGCAAAGG
PRKACB	CTCGGGACGGGTTCCTTTG	AGGGACGTATTCCATAACCATGT
MMP14	CAGTATGGCTACCTACCTCCAG	GCCTTGCCTGTCACTTGTAAA
miR-181a-5p	TTAGTGGCTGTCGCAACTTACAA	CATCTTCAAAGCACTTCCCT
miR-106b-5p	TGCGGCAACACCAGTCGATGG	CCAGTGCAGGGTCCGAGGT
miR-30c-5p	AGCGTCGTATCCAGTGCAAT	GTCGTATCCAGTGCGTGTCG
miR-30d-5p	GCCTGTAAACATCCCCGAC	GTGCGTGTCGTGGAGTCG
miR-30e-5p	TGTAAACATCCTTGACTGGAAGG	CCAGTGCGAATACCTCGGAC
miR-19a-3p	CGCTGTGCAAATCTATGCAAA	CAGTGTGCAAATCTATGCAA
miR-19b-3p	TGTCATAATCACTGTGCAAATCC	TATGGTTTTGACGACTGTGTGAT
miR-194-5p	GCGGCGGTGTAACAGAACTCC	ATCCAGTGCAGGGTCCGAGG
GAPDH	TGAAGGGTGGAGCCAAAAG	AGTCTTCTGGGTGGCAGTGAT
U6	AGAGCCTGTGGTGTCCG	CATCTTCAAAGCACTTCCCT

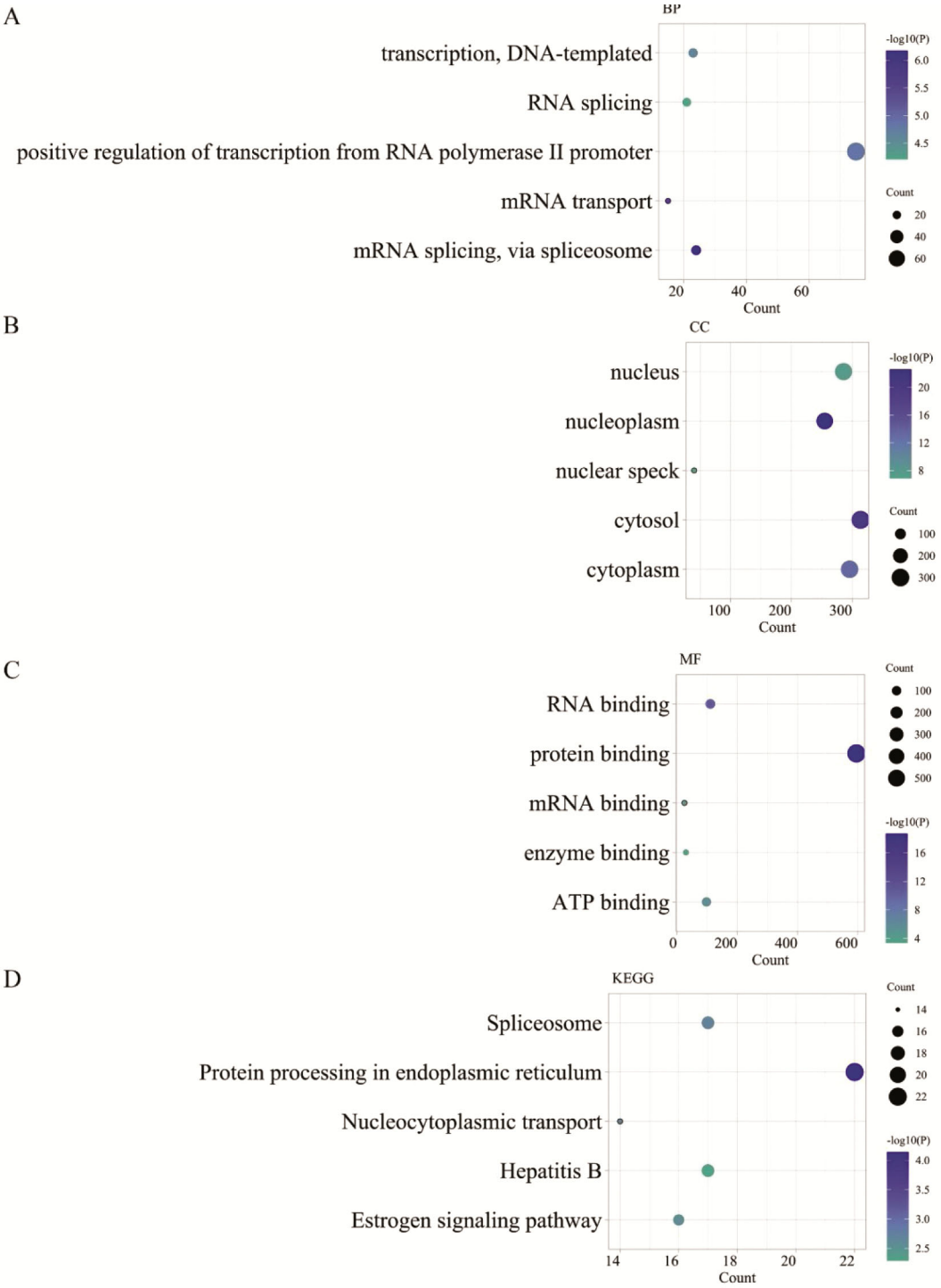

Fig. 1 — GO (A-C) and KEGG pathways (D) enrichment for GSE2208 DEGs. Bubble color indicates the P-value of enriched pathways, while bubble size corresponds to the number of genes

Identification and enrichment of DEGs in CD14+ monocytes

The GSE97498 contains human peripheral blood mononuclear cells and their derived osteoclasts. A total of 372 up-regulated and 866 down-regulated genes were identified according to specified inclusion and exclusion criteria. GO functional enrichment and KEGG pathway analyses were conducted to clarify the roles of DEGs, with the top 5 results displayed in (Fig. 2A-C) . BP included positive regulation of cell migration, cell migration, inflammatory response,

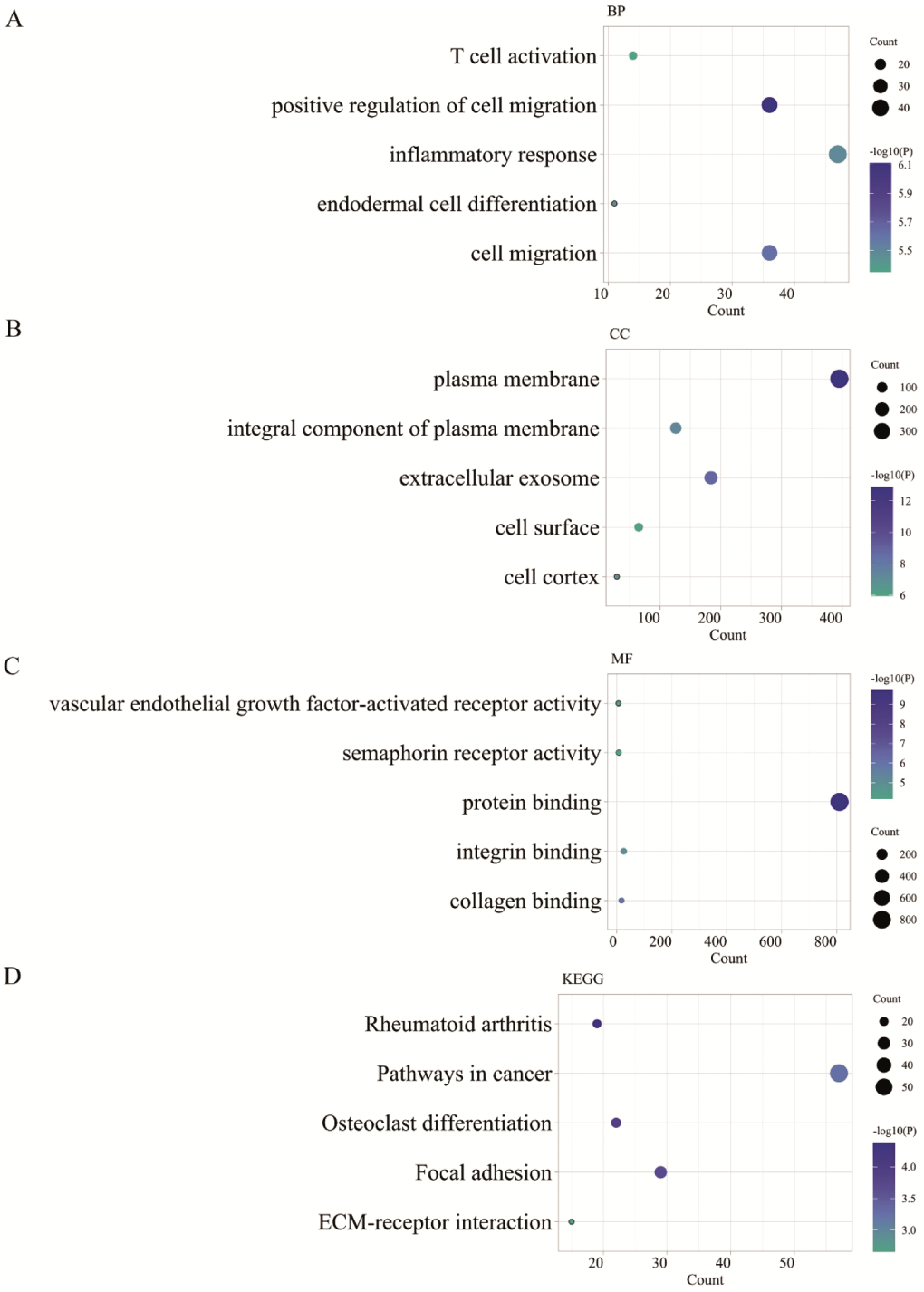

Fig. 2 — GO (A-C) and KEGG pathways (D) enrichment for GSE97498 DEGs. Bubble color indicates the P-value of enriched pathways, while bubble size corresponds to the number of genes

endodermal cell differentiation, and T cell activation; CC included plasma membrane, extracellular exosome, integral component of the plasma membrane, cell cortex, and cell surface; MF included protein binding, collagen binding, integrin binding, vascular endothelial growth factor-activated receptor activity, semaphorin receptor activity. KEGG pathway included rheumatoid arthritis, osteoclast differentiation, focal adhesion, pathways in cancer, and ECM-receptor interaction (Fig. 2D) .

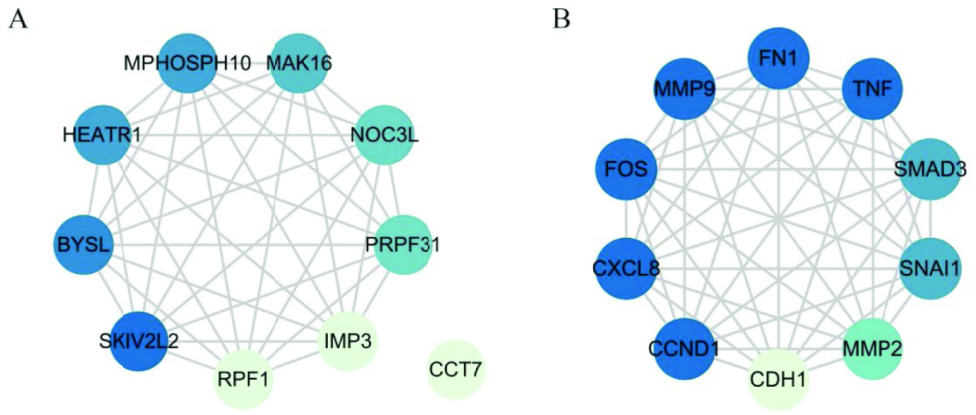

Fig. 3 — (A) Hub genes within the PPI network of DEGs in monocytes from individuals with high-PBM and low-PBM, (B) Hub genes identified in the PPI network of DEGs within CD14+ monocytes

PPI network analysis of DEGs in Low-PBM monocytes and CD14+ monocytes

The functional interaction network of the Low-PBM monocytes DEGs was obtained using string, which contains 681 nodes and 3773 interaction pairs. The functional interactive network of CD14+ monocytes DEGs obtained by string contains 1078 nodes and 5441 interactive pairs. Data were imported into Cytoscape for visualization. The cytoHubba in Cytoscape software was used to perform hub gene clustering. The top 10 nodes in MCC come together (Fig. 3A & B) .

Identification and clustering analysis of overlapping genes

A total of 58 overlapping genes were identified between 747 DEGs in high and low PBM monocytes and 1238 DEGs in CD14+ monocytes (Fig. 4A) . Cluster analysis was conducted to depict the interaction between overlapping genes. Gene clustering and network analysis were carried out with Cytoscape. Ten genes in monocytes, shown in (Fig. 4B) , were found to be significant in bone loss processes. Further, GO and KEGG pathway analyses of the ten hub genes were conducted via the DAVID online website (Fig. 4C-F) .

Prediction miRNA-Gene regulatory modules

Based on CyTargetLinker, a network with 333 nodes and 469 edges was constructed (Fig. 5A) . A total of 42 miRNAs were identified with an overlap threshold of 2. By analyzing GSE64433, DEmiRNA in osteoporosis patients were identified, and their intersection with 42 miRNAs predicted by CyTargetLinker resulted in 8 predicted miRNAs (miR-181a-5p, miR-106b-5p, miR-30c-5p, miR-30d-5p, miR-30e-5p, miR-19a-3p, miR-19b-3p, miR-194-5p) (Fig. 5B) . Specifically, miR-19a-3p and miR-19b-3p jointly regulate SOCS3 and PRKACB, six miRNAs regulate SOCS3, three miRNAs regulate PRKACB, two miRNAs regulate TNF, miR-194-5p regulates HBEGF, and miR-181a-5p regulates MMP14.

Validation of hub genes and predicted miRNAs *in vivo*

The OVX mice model was used to simulate postmenopausal osteoporosis (PMOP) and validate hub genes *in vivo*. Three months post-surgery, μ-CT analysis showed a significant decrease in trabecular bone number in the OVX group relative to the SHAM group, confirming the OVX model's validity (Fig. 6A & B) . Monocyte-derived mRNA and miRNA from whole blood were analyzed to evaluate hub genes and predicted miRNA expression levels. In the OVX group, RT-qPCR experiments indicated lower mRNA levels for six hub genes and higher levels for four hub genes relative to the SHAM group. Additionally, all eight miRNAs displayed increased expression in the OVX group relative to the SHAM group (Fig. 6C & D) . The hub genes and predicted miRNA expression were consistent with our bioinformatics analysis. This study indicates that hub genes and predicted miRNAs may serve as early diagnostic biomarkers for PMOP. Further research is necessary to uncover the specific mechanisms driving these observations.

Discussion

OP, a systemic bone disease, increases the risk of fragility fractures, pathological fractures, and muscle spasms, imposing a significant burden on patients' families and society[17]. Early screening and identification of risk factors can enable timely

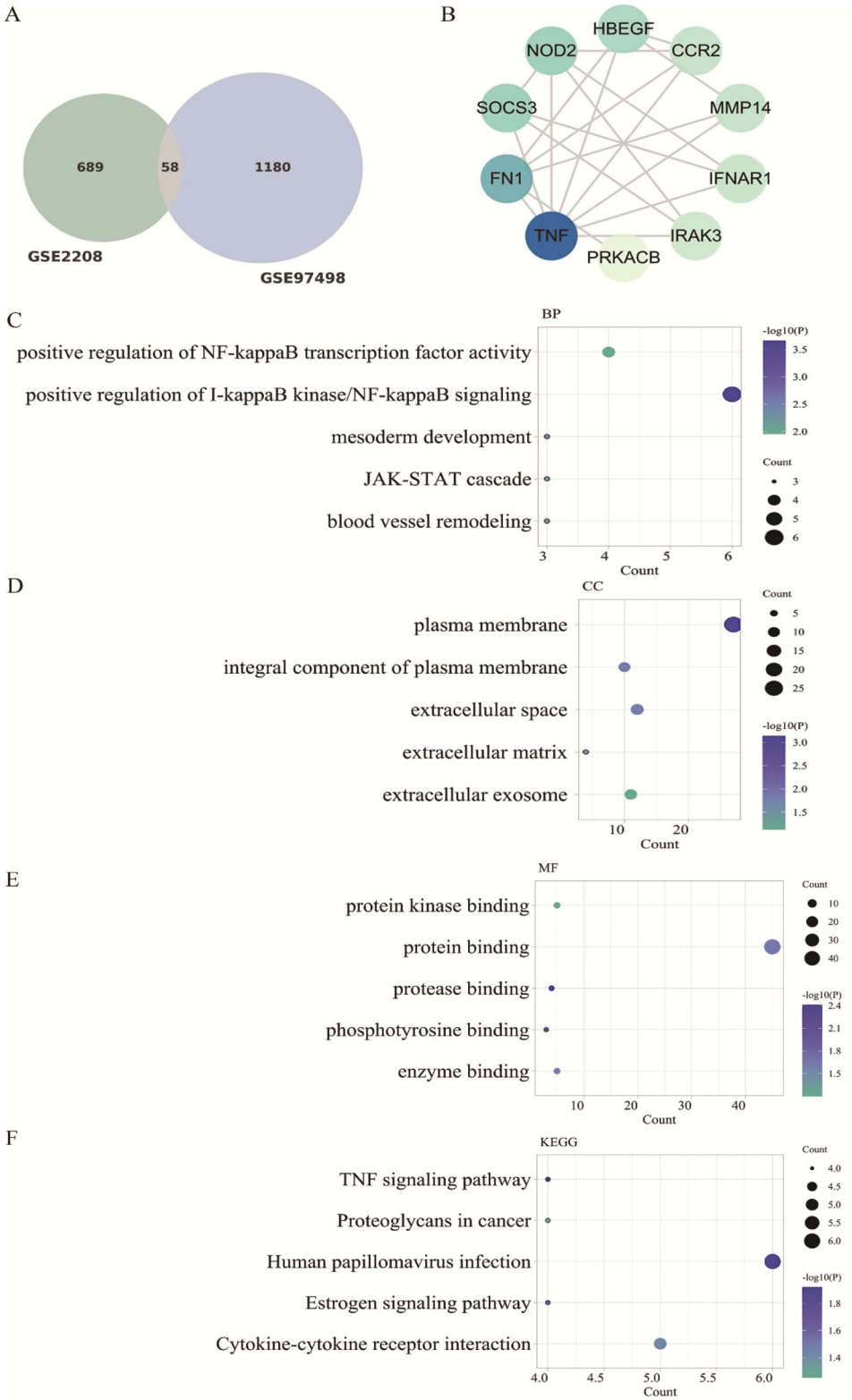

Fig. 4 — (A) The Venn diagram showing DEGs between high-PBM and low-PBM monocytes in GSE2208 and CD14+ monocytes in GSE97498; (B) Analysis of hub genes using cytoHubba for the overlapping genes. GO (C-E) and KEGG pathways (F) enrichment for the overlapping genes. Bubble color reflects the P-value of enriched pathways, while bubble size represents the number of associated genes

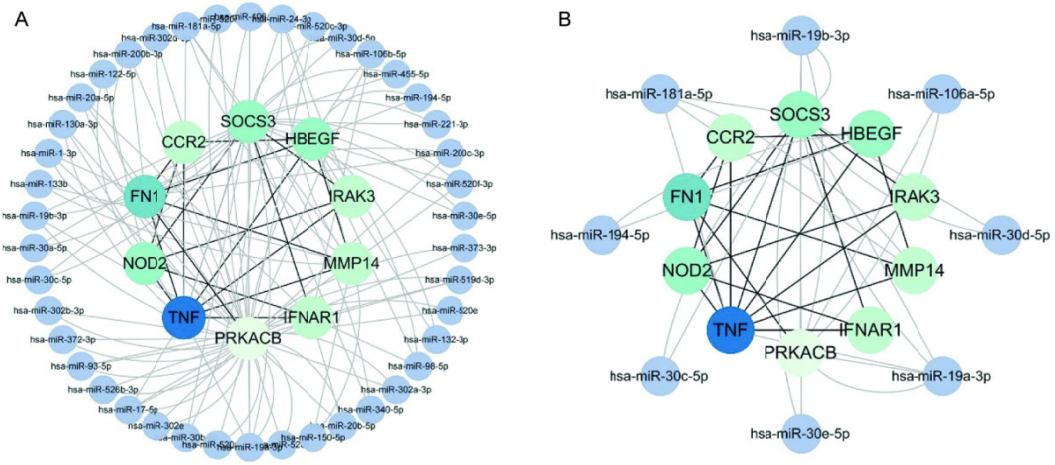

Fig. 5 — (A) 10 hub genes and their predicted miRNAs from CyTargetLinker extended network analysis; and (B) The regulation network connects ten hub genes and eight predicted miRNAs

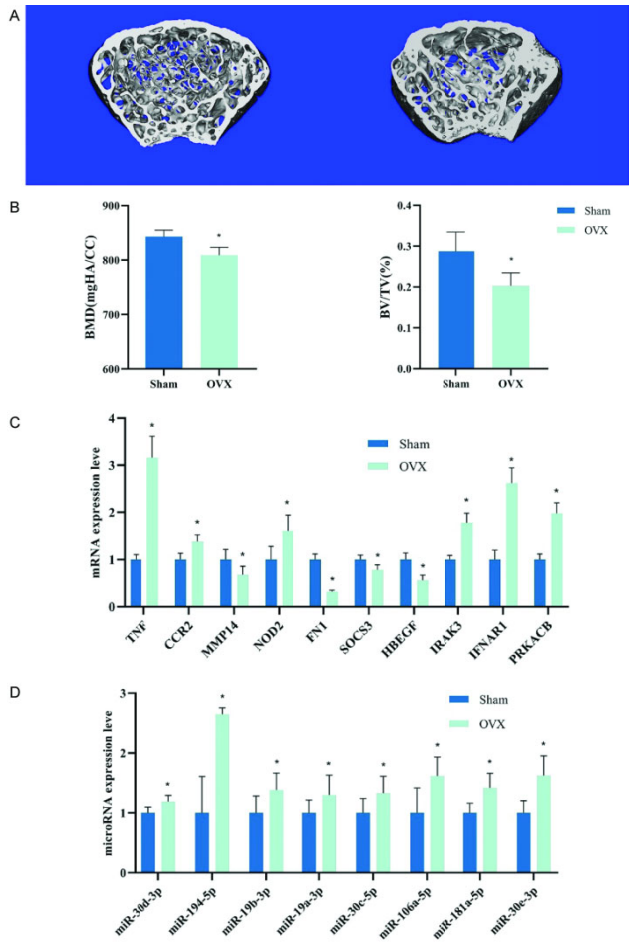

Fig. 6 — Validation of the hub genes and miRNAs *in vivo*. (A) Representative 3D Mimics reconstructed images of femurs from the SHAM group and OVX group of C57BL/6 mice; (B) Bone mineral density and BV/TV values of femurs in the SHAM and OVX groups; (C) mRNA expression levels of 10 hub genes in the SHAM and OVX groups; and (D) miRNA expression levels of 8 predicted miRNAs in the OVX group and SHAM group. Compared with the SHAM group, * $P< 0.05$

preventive measures; therefore, early diagnosis and intervention at the molecular level are of profound clinical significance. BMD is the most critical predictor and diagnostic indicator of osteoporosis[18]. Research indicates that attaining peak bone mineral density (PBMD) in adolescence decreases the risk of OP in adulthood[19]. In addition, Blood mononuclear cells, the precursors of osteoclasts, produce cytokines essential for the differentiation, activation, and apoptosis of osteoclasts. This study aims to identify early diagnostic biomarkers for osteoporosis in the population. In this study, 58 DEGs were filtered from two datasets. Ten hub genes were identified through PPI network analysis. Additionally, The biological roles of the DEGs were investigated through GO and KEGG enrichment analyses, and targeted miRNAs for the hub genes were predicted for further research.

Based on PPI, we identified the following hub genes: TNF, FN-1, CCR2, HB-EGF, MMP14, NOD2, SOCS3, IFNAR1, IRAK3, and PRKACB. Tumor necrosis factor-α (TNF-α) is a critical immune cytokine involved in inflammation and bone erosion in conditions linked to bone loss[20]. TNF has limited capacity to induce osteoclast precursor differentiation directly but works synergistically with RANKL to indirectly enhance osteoclastogenesis[21,22]. TNF indirectly enhances osteoclastogenesis by upregulating c-Fms and RANK expression in OC precursors and stimulating RANKL and M-CSF production in OBs. Research on bone destruction diseases like RA shows that RBP-J and the RBP-J/NFATC1-MIR182 regulatory pathway can block TNF-mediated OC differentiation and bone resorption without impairing RANKL-induced OC differentiation, maintaining bone remodeling and

advancing OP research[23,24]. Fibronectin 1 (FN-1) , part of the ligand glycoprotein family, is broadly expressed across cell types and interacts with cell surfaces and molecules like fibronectin, DNA, collagen, and actin[25]. FN-1 expression has been connected to arthritis and atherosclerosis[26]. According to Yang et al., through the WNT/β-catenin pathway, FN-1 enhances preosteoblast differentiation and mineralization, relying on ITGB1 for pathway activation. FN1 promotes collagen production and chondrocyte differentiation in femur fracture mice via the TGFβ/PI3K/Akt pathway[27]. Under mechanical stimulation, estrogen deficiency causes the FN1 network synthesized by osteoblasts to become loose and discontinuous, thereby affecting osteoblast function. CCR2, a CC chemokine receptor, is predominantly found in macrophages and inflammatory cells. The chemokine (CC Motif) ligand 2 (CCL2) interaction with CCR2 promotes osteoclast fusion and maturation. Blocking CCL2 or CCR2 decreases the quantity and activity of mature osteoclasts, reducing bone resorption[28]. Research demonstrated that CCR2-/- mice had stronger and larger tibias than wild-type controls. Still, after ovariectomy (OVX) and denervation (DEN) treatment, their tibial structure and function were similar, indicating that CCR2 knockout does not protect from bone loss. These findings imply that CCR2 may not be a reliable target for treating bone loss[29]. HB-EGF originates from the peptide growth factor family related to epidermal growth factor (EGF) . HB-EGF is found in multiple cell types and tissues, such as vascular endothelial cells, renal mesangial cells, skeletal muscle, keratinocytes, and inflammatory cells. HB-EGF signaling is associated with skeletal development. HB-EGF promotes BMSC proliferation *in vitro* by activating the Erk and Akt1 pathways. HB-EGF inhibits BMSC differentiation by inhibiting BMP-Smad1/5/8 signaling[30]. MMP14, a membrane-associated matrix metalloproteinase, is pivotal in inflammatory bone conditions. Increased expression of MMP14 in osteoclasts aids in collagen degradation and matrix protein breakdown, enhancing bone resorption. Studies have shown that MMP14 contributes to bone erosion in the c-Fos-deficient Sh3bp2KI/KI mice model by enhancing macrophage collagen degradation[31]. MMP14 participates in PTH-induced bone resorption through the regulation of soluble RANKL production. Suppressing MMP14 can protect the bone mass gains induced by PTH treatment. Future studies should focus on exploring the relationship between MMP14 and OP[32]. NOD2, a nucleotide-binding and oligomerization domain-like receptor (NLR) family member, is predominantly expressed in myeloid cells and regulates autophagy, immune responses, reactive oxygen species (ROS) production, and apoptosis. NOD2 contributes to ovariectomy-induced bone loss by triggering the NF-κB signaling pathway and elevating osteoclast ROS levels[33,34]. SOCS3 belongs to the suppressor of cytokine signaling (SOCS) family, which consists of intracellular proteins that provide negative feedback regulation. The JAK1/STAT3/SOCS3 signaling axis is a critical regulator in bone development, pathology, and physiology[35]. IL-6 promotes osteoclast formation by activating STAT3 signaling within the osteoblast lineage. SOCS3 acts as a negative feedback regulator for STAT3. Its deficiency results in excessive activation of the STAT3 signaling pathway, affecting bone metabolic balance[36,37]. IFNAR1, the interferon-alpha/beta receptor subunit 1, is crucial for regulating osteoclast differentiation[38]. IFNAR1 reduces c-Fos and NFATc1 expression through the action of type I interferons, mainly IFN-β. IFN-β specifically upregulates the chemokine CXCL11, which independently inhibits osteoclast differentiation, reinforcing its suppressive role[39]. IRAK3 serves as a key negative feedback regulator within the TLR/IL-1R signaling family. IRAK3 blocks NF-κB and MAPK pathway activation by preserving the IRAK-TRAF6 complex and halting the dissociation of IRAK from MyD88. IRAK3 deficiency increases bone resorption, indicating its protective role in bone metabolism. By reducing IRAK3 expression, glucocorticoids enhance osteoclast activity and bone resorption, which may be a key factor in glucocorticoid-induced osteoporosis[40,41]. PRKACB, a serine/threonine protein kinase, facilitates cAMP signal transduction, influencing cellular activities like differentiation, proliferation, and inflammation. MiR-302a-3p regulates the expression of RANKL in mandibular osteoblast-like cells through PRKACB inhibition. ZOL treatment suppresses RANKL expression by regulating the miR-302/PRKACB/RANKL signaling pathway. By downregulating RANKL expression, ZOL treatment can alleviate osteoporosis in HIV-positive patients undergoing tenofovir therapy[42-44].

In our study, we developed a PMOP mice model through bilateral oophorectomy. We observed reduced mRNA expression levels of FN-1, SOCS3, IRAK3, IFNAR1, PRKACB, and HB-EGF in the

OVX group relative to the SHAM group, while TNF, CCR2, MMP14, and NOD2 were upregulated, aligning with our bioinformatics results. The results from bioinformatics and animal experiments provide insights into the involvement of monocytes in premenopausal osteoporosis and identify ten potential PMOP biomarkers. We identified eight predicted miRNAs and their corresponding target genes. RT-qPCR experiments showed significant upregulation of 8 miRNAs in PBMCs from osteoporotic mice. The results indicate a positive relationship between these eight miRNAs and osteoporosis progression, implying their potential as biomarkers for osteoporosis.

Conclusion

A total of 58 overlapping DEGs and ten hub genes (TNF, FN-1, CCR2, HB-EGF, MMP14, NOD2, SOCS3, IFNAR1, IRAK3, PRKACB) were identified in this study. Additionally, miRNAs associated with the target genes were also identified. However, further research is necessary to establish the exact interactions between these genes and miRNAs. This study offers a set of valuable genes and miRNAs as potential biomarkers for the early screening of populations at high risk of osteoporosis.

Acknowledgement

This work was supported by the Basic and Applied Basic Research Foundation of Guangdong Province, China (2020A1515010435) , and by the Longgang District Medical and health science and technology project (LGKCYLWS20230024) .

Conflicts of interest

All authors declare no conflict of interest.

References

1 Ensrud KE & Crandall CJ, Osteoporosis. *Ann Intern Med*, 177 (2024) Itc1.
2 Gosset A, Pouillès JM & Trémollieres F, Menopausal hormone therapy for the management of osteoporosis. *Best Pract Res Clin Endocrinol Metab*, 35 (2021) 101551.
3 Ebeling PR, Nguyen HH, Aleksova J, Vincent A J, Wong P & Milat F, Secondary Osteoporosis. *Endocr Rev*, 43 (2022) 240.
4 Rizzoli R, Dairy products and bone health. *Aging Clin Exp Res*, 34 (2022) 9.
5 Rozenberg S, Bruyère O, Bergmann P, Cavalier E, Gielen E, Goemaere S, Kaufman JM, Lapauw B, Laurent M R, De Schepper J & Body JJ, How to manage osteoporosis before the age of 50. *Maturitas*, 138 (2020) 14.
6 Zhu X & Zheng H, Factors influencing peak bone mass gain. *Front Med*, 15 (2021) 53.
7 Akhiiarova K, Khusainova R, Minniakhmetov I, Mokrysheva N & Tyurin A, Peak Bone Mass Formation: Modern View of the Problem. *Biomedicines*, 11 (2023) .
8 Lv X, Gao F & Cao X, Skeletal interoception in bone homeostasis and pain. *Cell Metab*, 34 (2022) 1914.
9 Kim JM, Lin C, Stavre Z, Greenblatt MB & Shim JH, Osteoblast-Osteoclast Communication and Bone Homeostasis. *Cells*, 9 (2020) .
10 Søe K, Osteoclast Fusion: Physiological Regulation of Multinucleation through heterogeneity-potential implications for drug sensitivity. *Int J Mol Sci*, 21 (2020) .
11 Udagawa N, Koide M, Nakamura M, Nakamichi Y, Yamashita T, Uehara S, Kobayashi Y, Furuya Y, Yasuda H, Fukuda C & Tsuda E, Osteoclast differentiation by RANKL and OPG signaling pathways. *J Bone Miner Metab*, 39 (2021) 19.
12 Lademann F, Hofbauer LC & Rauner M, The Bone Morphogenetic Protein Pathway: The Osteoclastic Perspective. *Front Cell Dev Biol*, 8 (2020) 586031.
13 Patra BG, Maroufy V, Soltanalizadeh B, Deng N, Zheng WJ, Roberts K & Wu H, A content-based literature recommendation system for datasets to improve data reusability - A case study on Gene Expression Omnibus (GEO) datasets. *J Biomed Inform*, 104 (2020) 103399.
14 Ritchie ME, Phipson B, Wu D, Hu Y, Law CW, Shi W & Smyth GK, limma powers differential expression analyses for RNA-sequencing and microarray studies. *Nucleic Acids Res*, 43 (2015) e47.
15 Szklarczyk D, Gable AL, Lyon D, Junge A, Wyder S, Huerta-Cepas J, Simonovic M, Doncheva NT, Morris JH, Bork P, Jensen LJ & Mering CV, STRING v11: protein-protein association networks with increased coverage, supporting functional discovery in genome-wide experimental datasets. *Nucleic Acids Res*, 47 (2019) D607.
16 Doncheva NT, Morris JH, Holze H, Kirsch R, Nastou KC, Cuesta-Astroz Y, Rattei T, Szklarczyk D, von Mering C & Jensen LJ, Cytoscape stringApp 2.0: Analysis and Visualization of Heterogeneous Biological Networks. *J Proteome Res*, 22 (2023) 637.
17 Fischer V & Haffner-Luntzer M, Interaction between bone and immune cells: Implications for postmenopausal osteoporosis. *Semin Cell Dev Biol*, 123 (2022) 14.
18 Xiao P L, Cui A Y, Hsu C J, Peng R, Jiang N, Xu X H, Ma YG, Liu D & Lu HD, Global, regional prevalence, and risk factors of osteoporosis according to the World Health Organization diagnostic criteria: a systematic review and meta-analysis. *Osteoporos Int*, 33 (2022) 2137.
19 Zhang X, Yang L, Zhang J, Lix LM, Leslie WD, Kan B & Yang S, Secular Trends in Peak Bone Mineral Density: The National Health and Nutrition Examination Survey 1999-2018. *Calcif Tissue Int*, 114 (2024) 480.
20 Wang T & He C, TNF-α and IL-6: The Link between Immune and Bone System. *Curr Drug Targets*, 21 (2020) 213.
21 Yao Z, Getting SJ & Locke IC, Regulation of TNF-Induced Osteoclast Differentiation. *Cells*, 11 (2021) .
22 Zhao B, TNF and Bone Remodeling. *Curr Osteoporos Rep*, 15 (2017) 126.
23 Zhao B, Intrinsic Restriction of TNF-Mediated Inflammatory Osteoclastogenesis and Bone Resorption. *Front Endocrinol (Lausanne)* , 11 (2020) 583561.

24 Wu Y, Yang Y, Wang L, Chen Y, Han X, Sun L, Chen H & Chen Q, Effect of Bifidobacterium on osteoclasts: TNF-α/NF-κB inflammatory signal pathway-mediated mechanism. *Front Endocrinol (Lausanne)* , 14 (2023) 1109296.

25 Glasner A, Levi A, Enk J, Isaacson B, Viukov S, Orlanski S, Scope A, Neuman T, Enk CD, Hanna JH, Sexl V, Jonjic S, Seliger B, Zitvogel L & Mandelboim O, NKp46 Receptor-Mediated Interferon-γ Production by Natural Killer Cells Increases Fibronectin 1 to Alter Tumor Architecture and Control Metastasis. *Immunity*, 48 (2018) 107.

26 Yang J, Zhang Y, Liang J, Yang X, Liu L & Zhao H, Fibronectin-1 is a dominant mechanism for rheumatoid arthritis *via* the mediation of synovial fibroblasts activity. *Front Cell Dev Biol*, 10 (2022) 1010114.

27 Yang C, Wang C, Zhou J, Liang Q, He F, Li F, Li Y, Chen J, Zhang F, Han C, Liu J, Li K & Tang Y, Fibronectin 1 activates WNT/β-catenin signaling to induce osteogenic differentiation *via* integrin β1 interaction. *Lab Invest*, 100 (2020) 1494.

28 Sucur A, Jajic Z, Artukovic M, Matijasevic MI, Anic B, Flegar D, Markotic A, Kelava T, Ivcevic S, Kovacic N, Katavic V & Grcevic D, Chemokine signals are crucial for enhanced homing and differentiation of circulating osteoclast progenitor cells. *Arthritis Res Ther*, 19 (2017) 142.

29 Mader TL, Novotny S A, Lin AS, Guldberg RE, Lowe DA & Warren G L, CCR2 elimination in mice results in larger and stronger tibial bones but bone loss is not attenuated following ovariectomy or muscle denervation. *Calcif Tissue Int*, 95 (2014) 457.

30 Li P, Deng Q, Liu J, Yan J, Wei Z, Zhang Z, Liu H & Li B, Roles for HB-EGF in Mesenchymal Stromal Cell Proliferation and Differentiation During Skeletal Growth. *J Bone Miner Res*, 34 (2019) 295.

31 Kittaka M, Mayahara K, Mukai T, Yoshimoto T, Yoshitaka T, Gorski JP & Ueki Y, Cherubism Mice Also Deficient in c-Fos Exhibit Inflammatory Bone Destruction Executed by Macrophages That Express MMP14 Despite the Absence of TRAP+ Osteoclasts. *J Bone Miner Res*, 33 (2018) 167.

32 Delgado-Calle J, Hancock B, Likine EF, Sato AY, McAndrews K, Sanudo C, Bruzzaniti A, Riancho JA, Tonra JR & Bellido T, MMP14 is a novel target of PTH signaling in osteocytes that controls resorption by regulating soluble RANKL production. *Faseb J*, 32 (2018) 2878.

33 Ke K, Sul OJ, Chung SW, Suh JH & Choi HS, Lack of NOD2 attenuates ovariectomy-induced bone loss via inhibition of osteoclasts. *J Endocrinol*, 235 (2017) 85.

34 Soyocak A, Özgen M, Turgut Coşan D, Kurt H, Doğaner F, Armağan O, Değirmenci İ & Şahin Mutlu F, Genetic variation in NOD1/CARD4 and NOD2/CARD15 immune sensors and risk of osteoporosis. *Biosci Rep*, 40 (2020) .

35 Sims NA, The JAK1/STAT3/SOCS3 axis in bone development, physiology, and pathology. *Exp Mol Med*, 52 (2020) 1185.

36 McGregor NE, Walker EC, Chan AS, Poulton IJ, Cho EH, Windahl SH & Sims NA, STAT3 Hyperactivation Due to SOCS3 Deletion in Murine Osteocytes Accentuates Responses to Exercise- and Load-Induced Bone Formation. *J Bone Miner Res*, 37 (2022) 547.

37 Cho DC, Brennan HJ, Johnson RW, Poulton IJ, Gooi JH, Tonkin B A, McGregor N E, Walker E C, Handelsman DJ, Martin TJ & Sims NA, Bone corticalization requires local SOCS3 activity and is promoted by androgen action via interleukin-6. *Nat Commun*, 8 (2017) 806.

38 Kwon Y, Park OJ, Kim J, Cho J H, Yun C H & Han SH, Cyclic Dinucleotides Inhibit Osteoclast Differentiation Through STING-Mediated Interferon-β Signaling. *J Bone Miner Res*, 34 (2019) 1366.

39 Han B, Xie Q, Liang W, Yin P, Qu X & Hai Y, PLCG2 and IFNAR1: The Potential Biomarkers Mediated by Immune Infiltration and Osteoclast Differentiation of Ankylosing Spondylitis in the Peripheral Blood. *Mediators Inflamm*, 2024 (2024) 3358184.

40 Soares-Schanoski A, Gómez-Piña V, del Fresno C, Rodríguez-Rojas A, García F, Glaría A, Sánchez M, Vallejo-Cremades MT, Baos R, Fuentes-Prior P, Arnalich F & López-Collazo E, 6-Methylprednisolone down-regulates IRAK-M in human and murine osteoclasts and boosts bone-resorbing activity: a putative mechanism for corticoid-induced osteoporosis. *J Leukoc Biol*, 82 (2007) 700.

41 Li H, Cuartas E, Cui W, Choi Y, Crawford T D, Ke HZ, Kobayashi KS, Flavell RA & Vignery A, IL-1 receptor-associated kinase M is a central regulator of osteoclast differentiation and activation. *J Exp Med*, 201 (2005) 1169.

42 Irwandi RA, Khonsuphap P, Limlawan P & Vacharaksa A, miR-302a-3p regulates RANKL expression in human mandibular osteoblast-like cells. *J Cell Biochem*, 119 (2018) 4372.

43 Pemmari A, Leppänen T, Paukkeri EL, Eskelinen A, Moilanen T & Moilanen E, Gene expression in adverse reaction to metal debris around metal-on-metal arthroplasty: An RNA-Seq-based study. *J Trace Elem Med Biol*, 48 (2018) 149.

44 Lin W, Li XF, Ren DC, Song M, Duan L, Liu JZ & Zhan Z R, Administration of zoledronic acid alleviates osteoporosis in HIV patients by suppressing osteoclastogenesis *via* regulating RANKL expression. *Mol Med*, 27 (2021) 19.